Biogeosciences
Discussions

Open Access

EGU

1 **Ecosystem respiration in coastal tidal flats can be**

2 **modelled from air temperature, plant biomass and**

3 **inundation regime**

4 Xueyang Yu[1,2], Siyuan Ye[1,2*], Linda Olsson[3,4], Mengjie Wei[1,2], Ken W.

5 Krauss[5], Hans Brix[3,4]

6

7 1 Key Laboratory of Coastal Wetland Biogeosciences, China Geological Survey,

8   Qingdao Institute of Marine Geology, Qingdao, 266071, China;

9 2 Laboratory for Marine Geology, Qingdao National Laboratory for Marine Science and

10   Technology, Qingdao, 266061, China;

11 3 Aarhus University, Department of Bioscience, Aarhus, 8000C, Denmark;

12 4 Sino-Danish Centre for Education and Research, Aarhus, 8000C, Denmark;

13 5 U.S. Geological Survey, Wetland and Aquatic Research Center, Lafayette, Louisiana,

14   70506, United States of America.

15

16 Corresponding author's present address:

17 Qingdao Institute of Marine Geology, China Geological Survey, MLR

18 62 Fuzhou Road, Qingdao, China

19 Tel: 86-532-85755811

20 Fax: 86-532-85720553

21 Email: siyuanye@hotmail.com

22

23   Abstract

24   Ecosystem respiration contributes greatly to carbon emissions and losses

25   in coastal wetlands. To gain a better understanding of gaseous carbon loss from

26   a coastal wetland covered by seablite (*Suaeda salsa Pall.*) and to evaluate the

27   influence of environmental factors on ecosystem respiration, a multi-year in-situ

28   experiment was carried out during the growing season of 2012 through part of

29   2014. By partitioning total carbon dioxide (CO_2) flux into soil respiration (R_{soil})

30   and plant respiration (R_p), we found that during mid-summer, ecosystem CO_2

31   respiration rates (R_{eco}) were within the range of 844.5 to 1150.0 mg CO_2 m^{-2}

32   h^{-1}, while R_{eco} was as low as 31.7 to 110.8 mg CO_2 m^{-2} h^{-1} at the beginning

33   and the end of growing seasons. Aboveground *S. salsa* plant material

34   comprised 79.1% of total biomass on average, and R_p dominated R_{eco} during

35   inundated periods. It is estimated that 1 gram of soil-emergent *S. salsa* biomass

36   (dry weight) could produce approximately 1.41 to 1.46 mg CO_2 per hour during

37   mid-summer. When water level was below the soil surface, soil microbial and

38   belowground root respiration (R_{s+r}) was exponentially correlated with air

39   temperature. Based on our observation, an empirical model was developed to

40   estimate system respiration of the *S. salsa* marsh in the Liaohe River Delta,

41   Northeast China. This model can be applied for regional carbon budget

42   estimation purposes from *S. salsa* wetlands throughout Northeast China.

43

44   Keywords:

45   Coastal wetland, soil respiration, plant respiration, field observation,

46   carbon cycling, empirical modelling

Biogeosciences
Discussions

Open Access

EGU

1. Introduction

47

48   Coastal wetlands are known to sequester carbon at high rates, and many

49   are regulated by salinity to emit less methane than inland wetlands due to the

50   greater availability of sulfate (Chmura et al., 2003; Holm et al., 2016; Lu et al.,

51   2016). Ecosystem respiration (R_{eco}) is believed to be the dominant gaseous

52   carbon emissions process from coastal wetlands, weakening the carbon sink

53   function of coastal wetlands that have the highest effluxes of CO_2 (Nicholls,

54   2004; Smith et al., 1983). R_{eco} includes sources of CO_2 both routed through or

55   originating from emergent plant structures (R_p) and those sources associated

56   with soil microbial and belowground root respiration (R_{s+r}). R_p and R_{s+r} should

57   be quantified separately because each process has its unique seasonal pattern

58   and response to environmental factors (Li et al., 2010). Considering that CO_2

59   generated by plant and microbial respiration is much more than CO_2 generated

60   from anthropogenic activities (Raich et al., 2010), these fluxes from natural and

61   managed wetlands are inherently important in regulating the climate cycle in

62   providing positive feedbacks (i.e., greater CO_2 emissions; greater atmospheric

63   warming) or negative feedbacks (i.e., reduced CO_2 emissions; less atmospheric

64   warming) (Cox et al., 2000; Davidson and Janssens, 2006; Melillo et al., 2002;

65   Mitsch et al., 2008). Coastal wetlands have been the focus of much attention

66   since large amounts of carbon can be stored in tidal (known as "blue carbon")

67   and in inland non-tidal coastal wetlands, but with a notable reduction in net

68   gaseous CO_2 (and CH_4) emissions when managed properly (Chen et al., 2016;

69   Jankowski et al., 2017; Rodríguez et al., 2017; Wang et al., 2016).

70   R_{eco} in coastal wetlands is influenced by many environmental factors

71   including soil and air temperature (Arora et al., 2016; Juszczak et al., 2013),

72   soil properties (Hassink, 1992), salinity (Neubauer et al., 2013), plant type (Xu

73   et al., 2014), root biomass (Krauss et al., 2012), and hydrologic conditions

74   (Guan et al., 2011). Environmental factors change greatly with time, which

Biogeosciences
Discussions

75   create bias on evaluating R_{eco} if the full range of changing environmental

76   conditions is not included in determinations (Marínmuñiz et al., 2015; White et

77   al., 2014). In addition, R_p and soil microbial respiration have different responses

78   to temperature and water level change (Dawson and Tu, 2009; Hall and

79   Hopkins, 2015; Wu et al., 2017).

80   Our lack of understanding about CO_2 emissions from a wide range of

81   environments and environmental conditions results in difficulties in linking

82   response to key factors (Wolkovich et al., 2014), yet such linkages are critical

83   for modeling and determine area-scaled fluxes of use at regional and national

84   levels. Statistical analyses are useful in identifying interactions and the

85   importance of individual environmental factors in controlling R_{eco}, but such

86   information is often more locally relevant than globally and there has been

87   decidedly less quantification of larger-scale influence (Iwata et al., 2015; Song

88   et al., 2015). Modelling is an effective way to understand and evaluate CO_2

89   exchange between ecosystems and the atmosphere (Giltrap et al., 2010;

90   Kandel et al., 2013), given that empirical assessment often misses extreme

91   environmental conditions. By simulating biogeochemical activities, process-

92   based models are capable of interpreting material and energy flow from one

93   pool to another (Giltrap et al., 2010; Metzger et al., 2015; St-Hilaire et al., 2010).

94   However, as more processes are considered through iterative research, the

95   number of parameters of relevance to modelling can increase, which makes

96   models more complicated and more difficult to apply across scales (Wang and

97   Chen, 2012). Empirical models are easier to deploy for evaluating respiration

98   in the same ecosystem because driving variables are connected to

99   observations via mathematical formulas (Yuste et al., 2005). Biological

100   processes are not typically fully integrated within models, rather statistical

101   relationships are used to imply cause and effect, leading to imperfect model

102   structure and larger uncertainty in model projections (Larocque et al., 2008).

Biogeosciences
Open Access
Discussions
EGU

103   Partitioning in-situ R_{eco} into different components and determining the

104   variables controlling each component is challenging but important (Li et al.,

105   2010). For this approach, traditional chamber methods have advantages as flux

106   measurements are direct and linked over small spatial scales to environmental

107   measurements (Dyukarev, 2017; Pumpanen et al., 2004). This approach does

108   abandon a degree of reality accomplished through eddy covariance methods

109   (Aubinet et al., 2012; Nicolini et al., 2018). However, models can be applied

110   effectively to develop chamber-based assessments at larger scales.

111   *Suaeda salsa Pall* is a pioneer herbaceous species of tidal marshes and is

112   very tolerant to salinity (Baoshan et al., 2008; Guan et al., 2011). It naturally

113   grows on highly saline soil including intertidal zones of Europe and East Asia

114   as well as saline and alkaline soils of beaches and lakeshores in northern China.

115   The growing season R_{eco} rate of *S. salsa* wetlands in the Liaohe River Delta

116   and the Yellow River Delta averaged 335 to 402 mg CO_2 m^{-2} h^{-1} (Ye et al., 2016)

117   and approximately 193 mg CO_2 m^{-2} h^{-1} (Chen et al., 2016), respectively. From

118   these studies, temperature is believed the dominant controlling factor of R_{eco},

119   and several exponential correlations between temperature and R_{eco} have been

120   developed (Xie et al., 2014). However, water level also determines soil aerobic

121   versus anaerobic condition by enhancing or restricting oxygen availability,

122   respectively, and plant biomass also contributes to R_{eco} through emergent plant

123   structures and roots embedded below the soil surface (Olsson et al., 2015).

124   Due to a mix of temporal and spatial   characteristics of plant distributions and

125   environmental factors in *S. salsa* wetlands across their geographic range,

126   observing and measuring R_{eco} of *S. salsa* marshes across this range would be

127   cost-prohibitive (Sánchez-Cañete et al., 2017).

128   To gain a better understanding of gaseous carbon loss from a coastal

129   wetland covered by *S. salsa* and to evaluate the contributions of plant and soil

130   fluxes to R_{eco}, a multi-year in-situ experiment based on the chamber method

Biogeosciences
Discussions

131   was carried out during the growing seasons of 2102, 2013, and 2014. We

132   quantify the influence of temperature, biomass, and water table on ecosystem

133   respiration, as past studies, but we also develop a rapid assessment method

134   (ecosystem model) to estimate system-scale R_{eco} in *S. salsa* marshes of the

135   Liaohe River delta to aid future efforts to scale beyond where experimental

136   measurements are taken, and over potentially different environmental

137   conditions projected for the future. This rapid evaluation model also has

138   potential application in regional and national carbon budget estimation for *S.*

139   *salsa* wetlands with lower costs than direct empirical assessment.

140   ## 2.   Materials and methods

141   ### 2.1.   Study area

142   This study was conducted in the Liaohe Delta (121°25′–123°31′ E, 40°39′–

143   41°27′ N) of Northeast China (Figure 1). Natural wetlands in the Liaohe Delta

144   cover about 2610 km^2, which account for about 69% of the delta area (Ji et al.,

145   2009). In addition, rice agriculture (non-natural wetlands) comprises

146   approximately 3287 km^2, and is spread inside and outside of the Liaohe Delta

147   area proper. The Liaohe Delta is located in the temperate continental monsoon

148   zone with mean air temperature of 8.3 ℃, and a mean annual precipitation of

149   612 mm with most rain falling in summer. The mean annual evaporation rate is

150   1705 mm, and the mean annual sunshine duration is around 2769 h (Luo et al.,

151   2003). The average tidal range in the area is 2.7 m; tides are semi-diurnal. The

152   Liaohe Delta comprise what is believed to be the largest reed (*Phragmites*

153   *australis* Cav. Trin ex Steud) wetland in the world with a total area of

154   approximately 800 km^2 (Brix et al., 2014). A field study site was built 16 km west

155   of the Liaohe River mouth in a newly restored wetland on a former fallow tidal

156   flat colonized recently by *S. salsa*. *Saueda salsa* wetlands comprise only 32

157   km^2 in the Liaohe River delta, but provide seasonal color to the region during

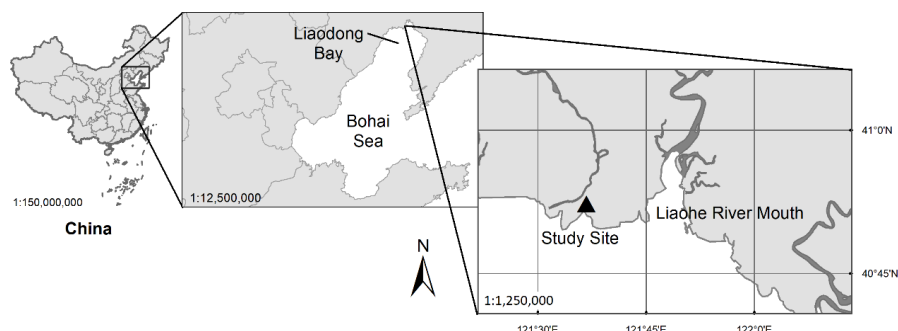158   flowering that draws tourists from all over China.

Biogeosciences
Discussions

Open Access

EGU

159

160   Figure 1 The location of the study site in the Liaohe Delta, Northeast China

161   The soil on the study sites is a silty clay loam with a sand, silt and clay

162   content of 20%, 65% and 15%, respectively, and a soil bulk density of

163   approximately 1.3 g cm^3. The soil total and organic carbon content are low,

164   averaging 9.5 g kg^{-1} and 6.4 g kg^{-1}, respectively, and total nitrogen content is

165   1.1 g kg^{-1}. Soil pH is 7.3 ± 0.4 (std. err.) and soil pore water salinity is 17 ± 2‰.

166   2.2. CO_2 flux measurements

167   The CO_2 fluxes were measured using a field-portable infrared gas analyzer

168   (Li-8100A, LI-COR Biosciences, Inc., Lincoln, NE, U.S.A.) with a commercial

169   survey chamber (8100-103). CO_2 measuring range was 0 to 3000 ppm with

170   errors less than 1.5 %. Circular survey collars (10 cm tall by 20 cm diameter)

171   were inserted 3 to 5 cm into the soil 2 hours before measurement began to limit

172   the influences of recent disturbance. The survey collar measured an area of

173   318 cm^2. The total volume of the flux chamber was calculated as the sum of the

174   volume of the commercial survey chamber system (~4843 cm^3) plus the volume

175   inside the collar factoring insertion depth of each collar individually. CO_2

176   concentrations were recorded at 1 Hz during 90 s measurement periods,

177   measurements were replicated twice, and values were averaged to ensure data

178   reproducibility (Mukhopadhyay and Maiti, 2014). Prior to each field trip, the

179   infrared gas analyzer was factory calibrated and checked for zero drift before

180   measurements using CO_2-free nitrogen gas (Dyukarev, 2017).

Biogeosciences
Discussions

Open Access

181   The CO_2 fluxes (F, mg CO_2 m^{-2} h^{-1}) were calculated according to the

182   following equation:

183
$$F = \frac{dc}{dt}\frac{M}{V_0}\frac{P}{P_0}\frac{T_0}{T}\frac{V}{S}$$

184   Where dc/dt (mol h^{-1}) is the slope of the linear regression line for CO_2

185   concentration over time; M (mg mol^{-1}) is the molecular mass of CO_2; P (in

186   Pascals) is the barometric pressure; T (in Kelvin) is the absolute temperature

187   during sampling; V (in Liters) is the total volume of the enclosure measuring

188   space; S (in m^2) is the cover area of the measuring plot. V_0 (22.4 L/mol), T_0

189   (273.15 K) and P_0 (101.3 kPa) are the gas mole volume, absolute air

190   temperature, and atmospheric pressure under standard condition, respectively

191   (Song et al., 2009).

192   2.3.   Experimental design

193   Fluxes of CO_2 were measured approximately monthly during the growing

194   seasons of 2012, 2013, and 2014 (figure 2), for a total of 15 months of

195   measurements over the three years. Soils of Liaohe Delta wetlands are frozen

196   to depths of 15 cm during the months of December to March (Ye et al., 2016).

197   Six plots were established, and all had different amounts of vegetation

198   coverage in each observation month. On each plot, three measuring

199   procedures were included, as follows:

200   (1) Measurement of the entire ecosystem CO_2 flux by including all

201   vegetation and soil area under that vagatation, "R_{eco}";

202   (2) Measurement of plant material after cutting and removing all *S. salsa*

203   at 1 to 2 cm above soil surface, R_p. We placed all *S. salsa* into a sealed and

204   dark survey collar immediately after harvest (within 2 minutes) and measured

205 CO_2 flux from the still physiologically active plants.

206   (3) Measurement of CO_2 flux within the survey chamber but without

207   standing plants, which indicates soil microbial respiration plus respiration of

208   roots underlying those soils, R_{s+r}. R_{s+r} was taken when soils were not inundated.

209   Additional measurements were taken when soils were inundated, and those

210   measurements used to partition CO_2 exchange between the water surface and

211   the atmosphere at those times.

212   All harvested *S. salsa* plant material was dried to a constant mass at 65 °C

213   in a convection oven for a measure of aboveground biomass (AGB). A 15 cm

214   deep surface soil sample was taken within each survey collar after

215   measurements were completed during each sampling period. Living roots of *S.*

216   *salsa* were collected, separated from the soil column and dried in an oven at

217   65°C to constant mass for a measure of belowground biomass (BGB).
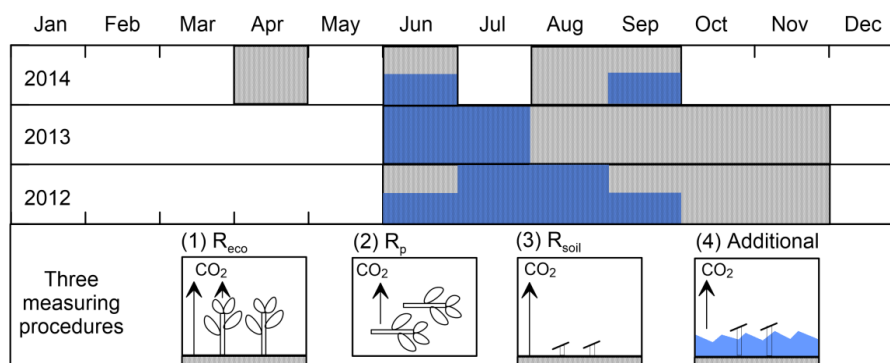
218

219   Figure 2 The observing period and procedures. The observation periods from 2012

220   to 2014 was marked as filled grey patches on the top subplot. Vertical blue patches

221   indicated the relative water level of a corresponding observation period. Months with

222   continuous blue rectangles refer to inundation of all six plots; half covered refer to

223   inundation of only some of the plots; and no blue bar equates to no inundation. The

224   bottom subplot displays a visual depiction of procedures. R_{eco}, R_{s+r}, and R_p were

225   measured in the corresponnding sequence.

226

227   2.4.   Statistical analysis and modeling

228   All monthly data are presented as means among plots with corresponding

229   standard errors among plots. Correlation analyses were conducted to examine

230   the relationships between the fluxes and the measured environmental variables.

231   In all tests, the differences were considered significant at $p < 0.05$. Least square

232   curve fitting was applied to quantify the influence of environmental factors. An

233   empirical model was developed using Spyder 3.2.4 on Python 3.6 platform

234   based on the field observations of respiration (R_{eco}) in various treatments and

235   their corresponding air temperature, plant biomass, and inundation regime.

3.   Results and discussions

3.1.   Ecosystem respiration

238   Overall, soil and root respiration (R_{s+r}) and plant respiration (R_p)

239   contributed 16% and 84%, respectively, to the total ecosystem respiration (R_{eco}).

240   However, the relative contributions of R_{s+r} and R_p varied both during the season

241   and between seasons (Figure 3).

242   R_{eco} varied significantly over the growing season with peak values in

243   August when the weather was hot (Figure 3). The seasonal pattern was nearly

244   identical between years, although peak R_{eco} varied between 845 mg CO_2 m^{-2}

245   h^{-1} in 2014 and 1150 mg CO_2 m^{-2} h^{-1} in 2013. During mid-summer (July and

246   August) there was great spatial variation in R_{eco} (as indicated by relatively large

247   variation among measurements) due to the variations in plant biomass within

248   the collars and also differences in water table depth at the time of specific

249   measurements.

250   R_{s+r} generally varied in concert with R_{eco} with highest rates in July-August,

251   except in 2012 where rates were low (< 100 mg CO_2 m^{-2} h^{-1}) in July and August.

252   This corresponds to a period where the soil surface in all six measuring plots

253   was inundated, i.e. had standing water on the soil surface. This was also the

254   case in June-July in 2013 which also had very low R_{s+r} rates. The inundation

255   probably reduces R_{s+r} because of the prevailing anoxic conditions in the soil

256   which is likely to occur as a consequence of the inundation. However, emission

257   of CO_2 to the atmosphere through the water surface might also be reduced

258   because CO_2 is highly soluble in water and enters into an equilibrium with the

259   bicarbonate buffer system (Berglund and Berglund, 2011), with is especially

260   prominent in saline water (i.e., the porewater of our sites was ~50% of full-

261   strength seawater). The highest soil respiration rates (>400 mg CO_2 m^{-2}) were

262   recorded in August of 2013 and 2014 where the water table was below the soil

263   surface and temperatures were high.

264   R_p generally peaked in August where temperatures were high and where

265   the plant biomass were maximal, except in 2014 where R_p was highest in

266   September. R_p generally varied in concert with R_{eco} and often, particularly

267   during inundated periods, contributed to most of the ecosystem respiration

268   (approximately 93 %), while both R_{s+r} and R_p contribute to R_{eco} when the water

269   table is below the soil surface (approximately 38 % R_{s+r} and 62 % R_p). R_{eco} from

270   additional *S. salsa* wetlands in the Liaohe Delta was in the range of what we

271   found, and also peaked in June to August, depending on the year (Ye et al.,

272   2016), corresponding strongly to peak seasonal aboveground biomass as well.

273   Our study confirms that all components of R_{eco} follow suit, with R_{s+r} and R_p

274   peaking concomitant with R_{eco} in most instances (figure 3), tracking plant growth.
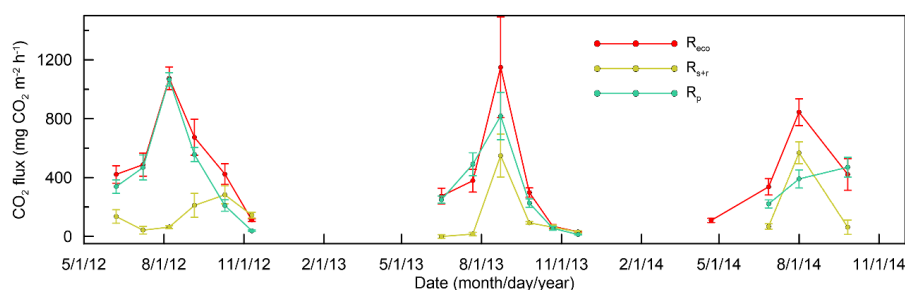

275

276   Figure 3. Seasonal variation in ecosystem respiration (R_{eco}), soil respiration (R_{s+r}),

277   and plant respiration (R_p) during the growing seasons of 2012-2014. . Errorbars are

278   standard error of the mean values.

279

280   3.2.   Plant biomass

281   *Suaeda salsa* is an annual herb that germinates and starts to grow in late

Biogeosciences
Discussions

282   April. The plants then follow the normal seasonal vegetation growth cycle for

283   cold temperate regions, with flowering beginning in July and maturation of

284   seeds occurring around late September (Mori et al., 2010). In the current study,

285   the biomass production of *S. salsa* largely followed this pattern reaching a total

286   biomass of between 530 and 930 g dry mass m^{-2} depending on year (Fig. 4).

287   Overall, the aboveground biomass constituted about 79% of the total biomass

288   (i.e., aboveground plus belowground), but the proportion varied during the

289   growing season. In the spring and early summer, the roots contributed a larger

290   proportion (25% to 35%) of the total biomass whereas in the late summer and

291   autumn the roots only constitute 15% to 20% of the total biomass. This shows

292   that the roots of *S. salsa* develop prior to peak above ground biomass, and are

293   thus slightly out of phase, suggesting an important role for early growing season

294   root growth initiation which also influences R_{eco}. After mid-September,

295   aboveground biomass remains stable probably because roots at this stage are

296   now able to support the biomass of the entire plant. Mao et al. (2011) reported

297   that the root covers 8%~13% of total *Suaeda salsa* biomass in the Yellow River

298   Delta, which was similar to our results.
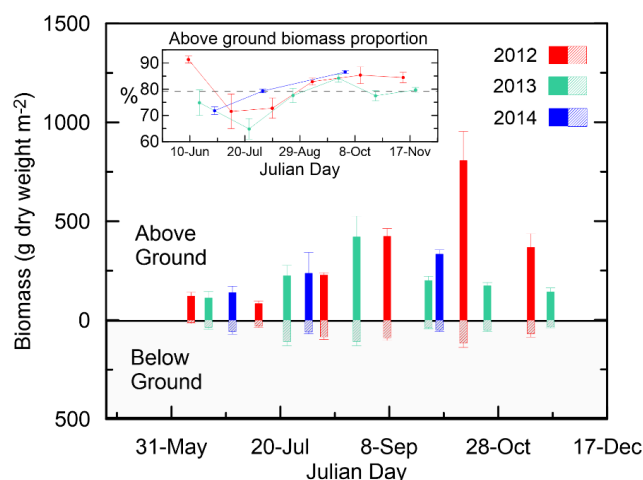
300   Figure 4 Seasonal variation of *S. Salsa* biomass during three growing seasons. Error

301   barsindicates the standard error at each sampling period (n=6). The inserted graph

Biogeosciences
Discussions

302   presents the proportion of aboveground biomass (AGB) of total biomass. The dashed line

303   indicates the overall average AGB proportion.

304   3.3.   Influencing environmental factors on R_{s+r} and R_p

305   Air temperature varied between 3°C and 33°C during the measuring period.

306   R_{s+r} rates were always low when the air temperature was below 18 ºC (Fig. 5),

307   which is consistent with the findings of Ye et al. (2016). When the low fluxes

308   measured during inundated periods were excluded, we found that R_{s+r} was

309   exponentially correlated with air temperature on a seasonal scale, which has

310   also been reported in several other studies (Bäckstrand et al., 2010; Xie et al.,

311   2014). If we did not remove fluxes of R_{s+r} that were measured during inundated

312   periods, the correlation would be significantly weakened (figure 5), suggesting

313   a strong statistical interaction between air temperature and inundation that

314   needs to be considered (Krauss et al., 2012). R_{eco} also correlated weakly with

315   air temperature probably because the combined effects of soil temperature,

316   water table, and plant biomass on R_{eco} were not considered (Flanagan et al.,

317   2002; Reth et al., 2005; Zhang et al., 2016). Observations from measuring plots

318   with large biomasses were significantly higher than the exponentially predicted

319   values, indicating that roots in the soils probably contributed significantly to R_{s+r}.
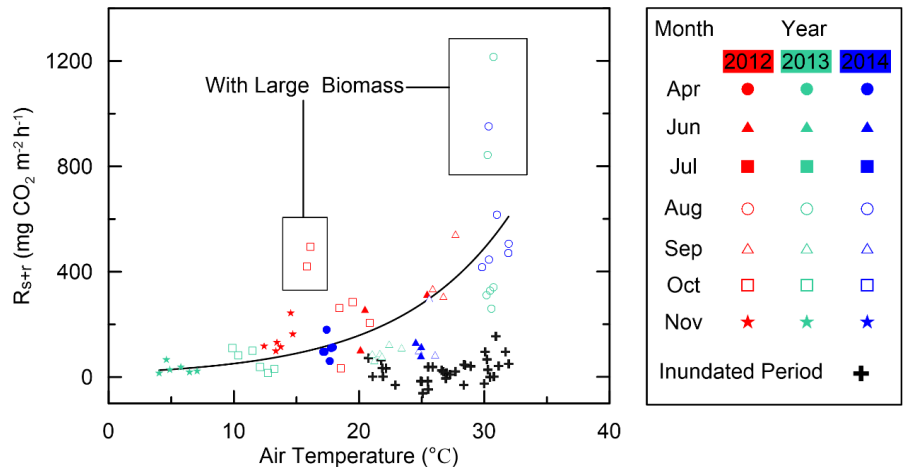
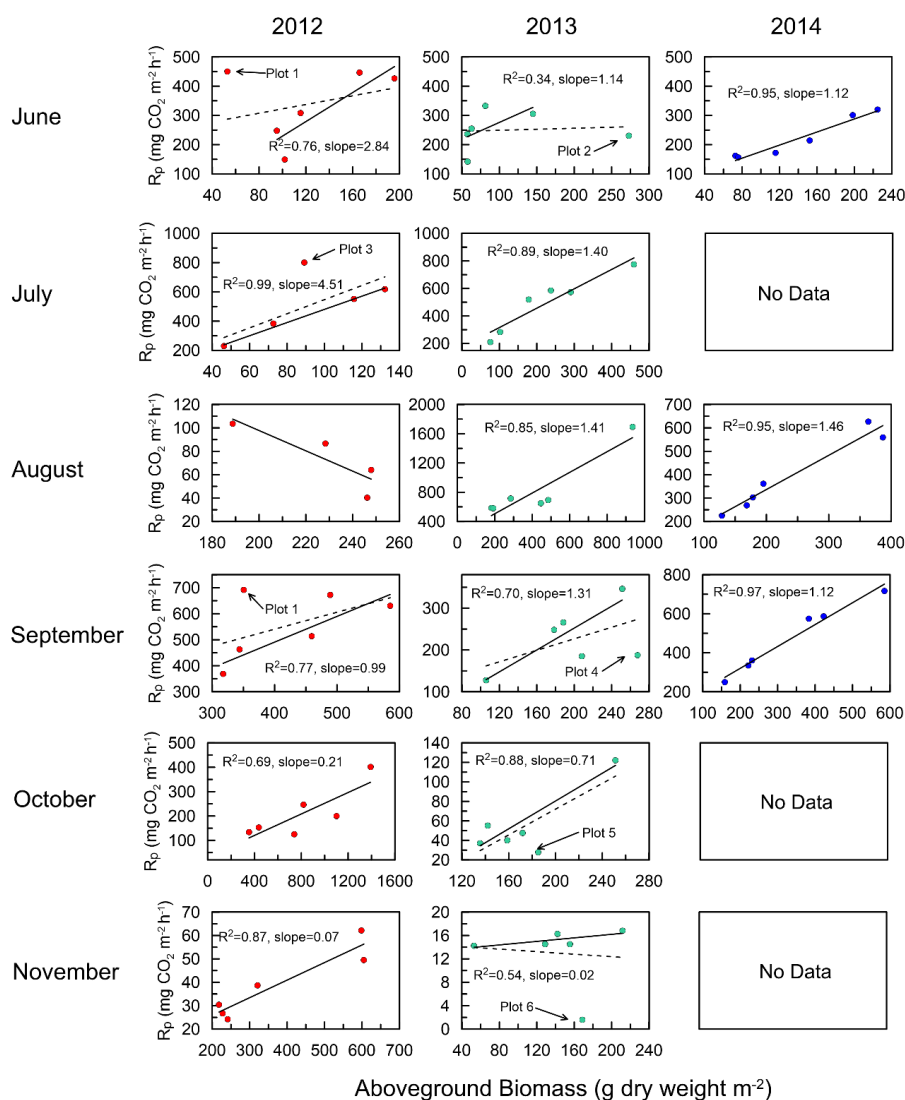321   Figure 5 The relationship between the observed soil respiration (R_{s+r}) rates and air

Biogeosciences
Discussions

Open Access

EGU

322   temperatures. The fluxes are grouped by month. The fluxes during inundated periods are

323   plotted separately using different marks (included in the correlation).

324   During inundated periods, R_{s+r} rates were low because water blocked both

325   oxygen and CO_2 transport (Yang et al., 2014). Water can both absorb or emit

326   CO_2 depending on the HCO_3^-/CO_3^{2-} balance in surface water and the dissolve

327   balance of CO_2 between surface water and the atmosphere (Wanninkhof and

328   Knox, 2003). *Suaeda salsa* has very limited aerenchyma in its tissue, and no

329   plant-mediated gas transport has been found in this species (Brix et al., 1996).

330   Besides, compared to the rates of R_{s+r} and R_p, the rates of gas exchange

331   between surface water and the atmosphere is low. Our observations suggest

332   that the main effect of inundation to the *S. salsa* marsh respiration is blocking

333   the gas transport from the soil to the atmosphere. Hence, the R_{s+r} rate is very

334   sensitive to water level variation just around the soil surface. This phenomenon

335   was also reported in cool temperate bog located in Mer Bleue, Canada (Lafleur

336   et al., 2005; Pugh et al., 2017).

337   Plants are reported to account for 35% to 90% of the total ecosystem

338   respiration in wetlands (Johnson et al., 2000), and are therefore believed to be

339   the dominant influencing factor for the spatial variation observed in R_{eco} (Han

340   et al., 2007). In the Yellow River delta, Han et al. (2014) did not find a significant

341   relationship between R_{eco} and biomass during the growing season in a *S. salsa*

342   wetland. This may be because they did not partition R_p, as we did here. As can

343   be seen in figure 3, R_p was close to R_{eco} during inundated periods, which shows

344   that the *S. salsa* plants contributed the most to the R_{eco}. In all periods except

345   August 2012, we observed a significant linear correlation between AGB and R_p

346   (figure 6). To demonstrate how the AGB influences R_p, the slope of the linear

347   curves versus Julian days are shown in figure 7. The slope of the regression

348   line varies over a growing season, and is < 0.1 mg CO_2 per g dry mass per hour

349   in October and November, probably because of plant senescence in the autumn.

350 The slopes obtained for 2013 and 2014 are comparable and the difference is

351 less than 5% in June and August. In June and July 2012, the slopes of R_p to

352 AGB are more than twice as high as the corresponding slopes of 2013 and

353 2014. As the study site was established in 2012, it is possible that the

354 biochemical conditions in the soil, including nutrient and organic carbon

355 concentrations, were disturbed slightly. The soil might have contained more

356 nutrients the first year, which might have led to high plant activity and

357 corresponding high respiration rates. Disregarding the larger slopes in 2012,

358 the remaining points follow a unimodal distribution over time. This can be

359 mathematically described by a Gaussian equation relating R_p/AGB over Julian

360 day (figure 7). Some studies prefer to use the air or soil temperature as the

361 proxy to evaluate seasonal parameters, while the accumulated temperature

362 has been shown to be better for evaluations of plant phenology (Cannell and

363 Smith, 1983). Since we did not measure meteorological variables on site

364 continuously over annual cycles, we are still able to predict respiration

365 parameters versus *S. salsa* plant biomass because of the significance of

366 seasonal time represented by Julian day as a proxy.

367

Aboveground Biomass (g dry weight m^{-2})

368   Figure 6   The relationship between plant respiration rate (R_p) and aboveground

369   biomass in each month during the three growing seasons. The linear correlation was

370   tested within each observation, the solid lines indicate the correlation after 'outlyers' are

371   removed, and the dashed line indicate the linear correlation with all data points included.

372
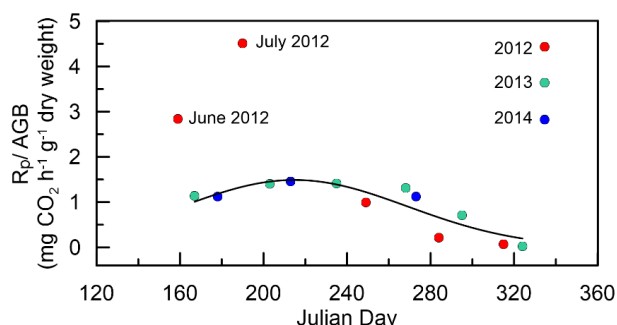
Figure 7 The seasonal variation of dry mass specific plant respiration rate (R_p/AGB).

The rate of June and July of 2012 are significantly higher than the other values, and are

thus not included in the seasonal variation estimation curve.

3.4. Modelling of components of ecosystem CO_2 fluxes

As is shown in Equation 1, R_{eco} is calculated as the sum of R_p and R_{s+r}.

$$R_{eco} = R_{s+r} + R_p \qquad \text{Equation 1}$$

3.4.1. Soil and root respiration

R_{s+r} was determined by water level and air temperature, which was

$$R_{s+r} = k_{WT} \times f(T) \qquad \text{Equation 2}$$

$$k_{WT} = \frac{e^{-ah}}{1+e^{-ah}} \qquad \text{Equation 3}$$

$$f(T) = F_0 \times e^{bT} \qquad \text{Equation 4}$$

Where k_{WT} represents the influence factor of water table, and $f(T)$ indicates

the influence of air temperature (T in °C) on R_{s+r} (figure 9). Equation 3 displays

the influence of water level on k_{WT}, with the parameter, a, a constant, indicating

the changing rate of water level (h in cm) relative to the soil surface on our study

sites. Here, a was determined to be 4.6, indicating that water level of 1cm could

block completely block the soil respiration, while -1 cm water level could provide

full R_{s+r} compacities (figure 10). Equation 4 indicates the relationship between

air temperature and R_{s+r} during non-inundated periods, which is represented by

an exponential curve (figure 5). Parameter b describes the temperature

sensitivity of R_{s+r} and F_0 (in mg CO_2 m^{-2} h^{-1}) was determined by R_{s+r} at 0 °C.

Biogeosciences

Discussions

Open Access

EGU

394 ### 3.4.2.   Plant respiration

395 R_p in *S. salsa* wetlands can be determined by

396 $$R_p = m_p \times k_{act}$$ Equation 5

397 where m_p (g dry weight m^{-2}) is the biomass of *S. salsa* and k_{act} was the

398 amount of CO_2 that 1 gram plant material can produce in 1 hour based on our

399 study, and is used here to indicate the influence that seasonal plant activity has

400 on R_p.

401 $$k_{act} = k_{amax} \times e^{-\left(\frac{D-D_m}{D_s}\right)^2}$$ Equation 6

402 k_{act} has a seasonal signature as well, related to environmental variables

403 such as air temperature; however, air temperatures alone were not as useful in

404 predicting R_p as k_{act}. A gaussian equation driving by Julian day was used to

405 evaluate the seasonal and annual variation in k_{act}. According to our observation

406 and analysis, the best fit parameters of k_{amax}, D_m, and D_s was 1.49, 214.83, and

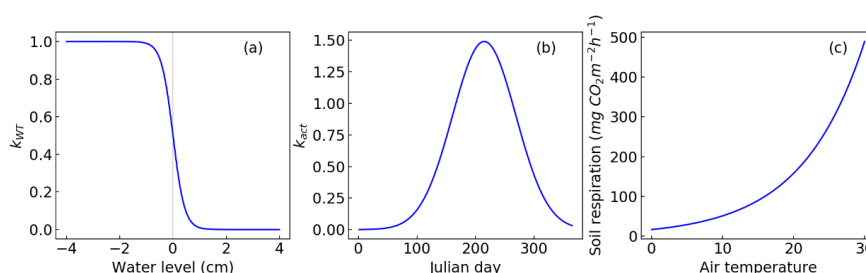407 76.63, respectively (figure 7, figure 8b).

408

409 Figure 8 Key parameters and the driving variables. (a): Parameter k_{WT} changes driven by

410 water level change near soil surface; (b): Seasonal variation of k_{act} driven by Julian day of

411 a year; (c): Soil respiration under different air temperatures.

412 As is shown in figure 9, R_{eco} in 2012 was significantly underestimated

413 because plant activity in 2012 was higher than the other two years (figure 4).

414 The estimated R_{s+r} rate includes living root respiration as well as soil organic

415 matter respiration (microbial) according to our model, if we assume the living

416 roots respire as fast as the aboveground parts. With the record of belowground

417 biomass and the parameter k_{act}, the contribution of each component can be

418   estimated. On our study sites, R_{s+r} had an average contribution of 23.9% to total

419   ecosystem respiration during the entire growing season. Knowing that the

420   modelled aboveground R_p covers an average of 55.2% of R_{eco}, plant biomass

421   determines the spatial variation in R_{eco}, and is therefore suggestive that our

422   model is widely applicable to other cold temperate *S. salsa* wetlands through

423   plant biomass, water table depth, and air temperature modeling alone. As

424   Moore and Dalva (1993) reported, the effects of climatic change on gas flux

425   from peatlands are more likely to be associated with changes in the water table

426   than with changes in thermal regime. The schematic respiration model derived

427   from our results follow suit (figure 10).
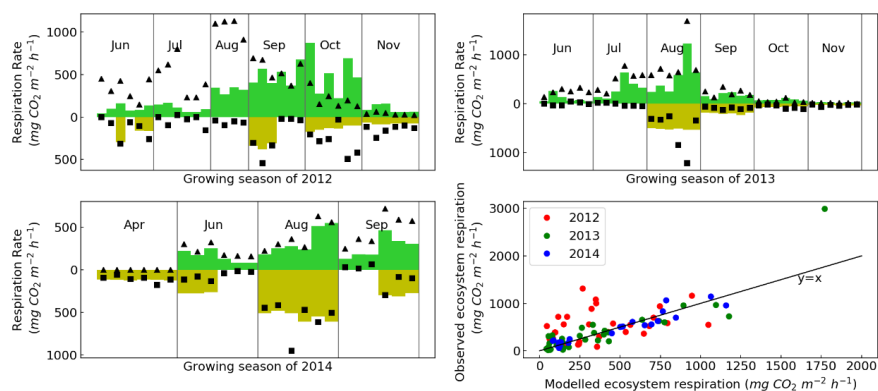
428

429   Figure 9 The observed respiration and modelled resiration. The triangle marks

430   represent observed R_p while the square marks represent observed R_{s+r}. The green and

431   tawny bars indicate the modelled R_p and R_{s+r}, respectively. The modelled and observed

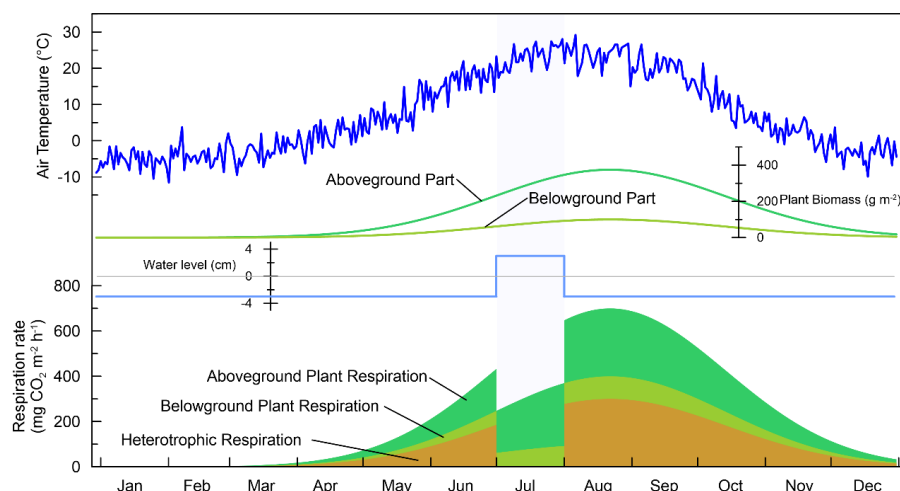432 R_{eco} of 2012, 2013 and 2014 are colored red, green and blue, respectively.

433

Figure 10   Schematic seasonal variation of ecosystem respiration and

environmental factors in *S.Salsa* marsh of the Liaohe River delta. Water level in July is

manully set above soil serface.

More complicated environmental variables (such as water table and

temperature) on plant activity, processes of gas diffusion and water HCO_3^-/CO_3^{2-}

balance are not included in this model due to the limitation of our field

observation. Besides, for only one dataset, comparing the observed data and

modelled data here makes less sense. More observations or data from other *S.*

salsa wetlands are needed to test this model on a larger scale. However, with

easily obtained environmental variables (AGB, air temperature, and water

regime), R_{eco} (and by extension R_p and R_{s+r}) rate can be estimated on a large

scale, making assessments of area-scaled CO_2 emissions from this wetland

type, such as conducted by Ye et al. (2016), more cost-effective in the future.

This model provides a regional rapid assessment protocol for R_{eco} within *S.*

salsa marshes; Necessary environmental variables can even be obtained

through remote sensing.

4. Conclusions

Ecosystem respiration (R_{eco}) of a *S. salsa* wetland in the Liaohe Rive Delta,

China, was observed to range from −61 to 2995 mg CO_2 m^{-2} h^{-1}, with significant

Biogeosciences
Discussions

Open Access

EGU

454   seasonal variation. Flux partitioning confirmed that R_{eco} was correlated with

455   plant biomass, water regime, and air temperature. Plant biomass and plant

456   activity controlled plant respiration, and further dominated the R_{eco} during

457   inundated period. Both soil and plant contributed to R_{eco} when water level was

458   below soil surface. Soil and root respiration is exponentially correlated with air

459   temperature with a sensitivity of 0.113 °C^{-1}. Besides, *S. salsa* could produce as

460   much as 1.41 to 1.46 mg CO_2 g^{-1} dry weight h^{-1} during mid-summer. Air

461   temperature, plant biomass, and hydrological regime are essential to estimate

462   R_{eco} using our proposed rapid assessment method. With regional data

463   calculated from remote sensing, the method can be used to evaluate R_{eco} of *S.*

464   *salsa* marshes on a large scale in the Liaohe River Delta, and potentially in

465   other similar cold temperate wetland types.

466   5. Acknowledgement

Biogeosciences
Discussions

Open Access

EGU

482   Panjin City for the help and convenience they offered. Finally, we thank all the

483   guides and suggestions to improve our manuscripts.

484   ## 6. References

485   Arora, B. et al., 2016. Influence of hydrological, biogeochemical and
486   temperature transients on subsurface carbon fluxes in a flood plain
487   environment. Biogeochemistry, 127(2): 1-30.
488   Aubinet, M., Vesala, T. and Papale, D., 2012. Eddy Covariance: A Practical
489   Guide to Measurement and Data Analysis. Springer: 365-376.
490   Bäckstrand, K. et al., 2010. Annual carbon gas budget for a subarctic peatland,
491   Northern Sweden. Biogeosciences, 7(1): 95-108.
492   Baoshan, C., Qiang, H. and Xinsheng, Z., 2008. Ecological thresholds of
493   Suaeda salsa to the environmental gradients of water table depth and soil
494   salinity. Acta Ecologica Sinica, 28(4): 1408-1418.
495   Berglund, Ö. and Berglund, K., 2011. Influence of water table level and soil
496   properties on emissions of greenhouse gases from cultivated peat soil. Soil
497   Biology & Biochemistry, 43(5): 923-931.
498   Brix, H., Sorrell, B.K. and Schierup, H.-H., 1996. Gas fluxes achieved by in situ
499   convective flow in *Phragmites australis*. Aquatic Botany, 54(2): 151-163.
500   Brix, H. et al., 2014. Large-scale management of common reed, Phragmites
501   australis , for paper production: A case study from the Liaohe Delta, China.
502   Ecological Engineering, 73: 760-769.
503   Cannell, M. and Smith, R.I., 1983. Thermal time, chill days and prediction of
504   budburst in Picea sitchensis. Journal of Applied Ecology, 20(3): 951-963.
505   Chen, L. et al., 2016. Effects of environmental and biotic factors on soil
506   respiration in a coastal wetland in the Yellow River Delta, China. Chinese
507   Journal of Applied Ecology, 27(6): 1795-1803.
508   Chmura, G.L., Anisfeld, S.C., Cahoon, D.R. and Lynch, J.C., 2003. Global
509   carbon sequestration in tidal, saline wetland soils. Global biogeochemical
510   cycles, 17(4): 1111-1132.
511   Cox, P.M., Betts, R.A., Jones, C.D., Spall, S.A. and Totterdell, I.J., 2000.
512   Acceleration of global warming due to carbon-cycle feedbacks in a coupled
513   climate model. Nature, 408(6809): 184-187.
514   Davidson, E.A. and Janssens, I.A., 2006. Temperature sensitivity of soil carbon
515   decomposition and feedbacks to climate change. Nature, 440(7081): 165-
516   173.
517   Dawson, T.E. and Tu, K.P., 2009. Partitioning Respiration Between Plant and
518   Microbial Sources Using Natural Abundance Stable Carbon Isotopes. Agu
519   Fall Meeting Abstracts.
520   Dyukarev, E.A., 2017. Partitioning of net ecosystem exchange using chamber
521   measurements data from bare soil and vegetated sites. Agricultural and

Biogeosciences
Discussions

Open Access

EGU

522   Forest Meteorology, 239: 236-248.

523 Flanagan, L.B., Wever, L.A. and Carlson, P.J., 2002. Seasonal and interannual
524   variation in carbon dioxide exchange and carbon balance in a northern
525   temperate grassland. Global change biology, 8(7): 599-615.

526 Giltrap, D.L., Li, C. and Saggar, S., 2010. DNDC: A process-based model of
527   greenhouse gas fluxes from agricultural soils. Agriculture, Ecosystems &
528   Environment, 136(3–4): 292-300.

529 Guan, B. et al., 2011. Physiological Responses of Halophyte Suaeda salsa to
530   Water Table and Salt Stresses in Coastal Wetland of Yellow River Delta.
531   Clean – Soil Air Water, 39(12): 1029–1035.

532 Hall, S. and Hopkins, D.W., 2015. A microbial biomass and respiration of soil,
533   peat and decomposing plant litter in a raised mire. Plant Soil &
534   Environment, 61(9): 405-409.

535 Han, G. et al., 2014. Ecosystem photosynthesis regulates soil respiration on a
536   diurnal scale with a short-term time lag in a coastal wetland. Soil Biology &
537   Biochemistry, 68(1): 85-94.

538 Han, G. et al., 2007. Soil temperature and biotic factors drive the seasonal
539   variation of soil respiration in a maize (Zea mays L.) agricultural ecosystem.
540   Plant & Soil, 291(1-2): 15-26.

541 Hassink, J., 1992. Effects of soil texture and structure on carbon and nitrogen
542   mineralization in grassland soils. Biology & Fertility of Soils, 14(2): 126-134.

543 Holm, G.O. et al., 2016. Ecosystem Level Methane Fluxes from Tidal
544   Freshwater and Brackish Marshes of the Mississippi River Delta:
545   Implications for Coastal Wetland Carbon Projects. Wetlands, 36(3): 401-
546   413.

547 Iwata, H. et al., 2015. Methane exchange in a poorly-drained black spruce
548   forest over permafrost observed using the eddy covariance technique.
549   Agricultural and Forest Meteorology, 214-215: 157-168.

550 Jankowski, K.L., Törnqvist, T.E. and Fernandes, A.M., 2017. Vulnerability of
551   Louisiana's coastal wetlands to present-day rates of relative sea-level rise.
552   Nature Communications, 8: 14792.

553 Ji, Y., Zhou, G. and New, T., 2009. Abiotic Factors Influencing the Distribution
554   of Vegetation in Coastal Estuary of the Liaohe Delta, Northeast China.
555   Estuaries and Coasts, 32(5): 937-942.

556 Johnson, L.C. et al., 2000. Plant carbon-nutrient interactions control CO_2
557   exchange in Alaskan wet sedge tundra ecosystems. Ecology, 81(2): 453-
558   469.

559 Juszczak et al., 2013. Ecosystem respiration in a heterogeneous temperate
560   peatland and its;sensitivity to peat temperature and water table depth.
561   Plant & Soil, 366(1-2): 505-520.

562 Kandel, T.P., Elsgaard, L. and Lærke , P.E., 2013. Measurement and modelling
563   of CO2 flux from a drained fen peatland cultivated with reed canary grass

Biogeosciences
Discussions

Open Access

EGU

564   and spring barley. Global Change Biology Bioenergy, 5(5): 548–561.

565   Krauss, K.W., Whitbeck, J.L. and Howard, R.J., 2012. On the relative roles of
566   hydrology, salinity, temperature, and root productivity in controlling soil
567   respiration from coastal swamps (freshwater). Plant & Soil, 358(1-2): 265-
568   274.

569   Lafleur, P.M., Moore, T.R., Roulet, N.T. and Frolking, S., 2005. Ecosystem
570   respiration in a cool temperate bog depends on peat temperature but not
571   water table. Ecosystems, 8(6): 619-629.

572   Larocque, G.R. et al., 2008. Uncertainty and Sensitivity Issues in Process-
573   based Models of Carbon and Nitrogen Cycles in Terrestrial Ecosystems.
574   Elsevier Science & Technology.

575   Li, X., Fu, H., Guo, D., Li, X. and Wan, C., 2010. Partitioning soil respiration and
576   assessing the carbon balance in a Setaria italica (L.) Beauv. Cropland on
577   the Loess Plateau, Northern China. Soil Biology and Biochemistry, 42(2):
578   337-346.

579   Lu, W. et al., 2016. Contrasting ecosystem CO_2 fluxes of inland and coastal
580   wetlands: A meta‐analysis of eddy covariance data. Global change
581   biology, 23(3): 1180-1198.

582   Luo, H., Huang, F. and Zhang, Y., 2003. Space-time change of marsh wetland
583   in Liaohe delta area and its ecological effect. Journal of Northeast Normal
584   University, 35.

585   Mao, P. et al., 2011. Biomass allocation in Suaeda salsa population in different
586   habitats of coastal zone. Ecology & Environmental Sciences, 20: 1214-
587   1220.

588   Marínmuñiz, J.L., Hernández, M.E. and Morenocasasola, P., 2015.
589   Greenhouse gas emissions from coastal freshwater wetlands in Veracruz
590   Mexico: Effect of plant community and seasonal dynamics. Atmospheric
591   Environment, 107(3): 107-117.

592   Melillo, J.M. et al., 2002. Soil warming and carbon-cycle feedbacks to the
593   climate system. Science, 298(5601): 2173-6.

594   Metzger, C. et al., 2015. CO_2 fluxes and ecosystem dynamics at five European
595   treeless peatlands–merging data and process oriented modeling.
596   Biogeosciences, 12(1): 125-146.

597   Mitsch, W.J. et al., 2008. Tropical wetlands for climate change research, water
598   quality management and conservation education on a university campus
599   in Costa Rica. Ecological Engineering, 34(4): 276-288.

600   Moore, T. and Dalva, M., 1993. The influence of temperature and water table
601   position on carbon dioxide and methane emissions from laboratory
602   columns of peatland soils. Journal of Soil Science, 44(4): 651-664.

603   Mori, S. et al., 2010. Physiological role of sodium in the growth of the halophyte
604   Suaeda salsa (L.) Pall. under high-sodium conditions. Crop Science, 50(6):
605   2492.

606   Mukhopadhyay, S. and Maiti, S.K., 2014. Soil CO_2 flux in grassland, afforested
607   land and reclamine overburden dumps: a case study. Land Degradation &
608   Development, 25(3): 216-227.
609   Neubauer, S.C., Franklin, R.B. and Berrier, D.J., 2013. Saltwater intrusion into
610   tidal freshwater marshes alters the biogeochemical processing of organic
611   carbon. Biogeosciences, 10(12): 8171-8183.
612   Nicholls, R.J., 2004. Coastal flooding and wetland loss in the 21st century:
613   changes under the SRES climate and socio-economic scenarios. Global
614   Environmental Change, 14(1): 69-86.
615   Nicolini, G. et al., 2018. Impact of CO_2 storage flux sampling uncertainty on net
616   ecosystem exchange measured by eddy covariance. Agricultural and
617   Forest Meteorology, 248(Supplement C): 228-239.
618   Olsson, L. et al., 2015. Factors influencing CO_2 and CH_4 emissions from coastal
619   wetlands in the Liaohe Delta, Northeast China. Biogeosciences, 12(16):
620   4965-4977.
621   Pugh, C.A., Reed, D.E., Desai, A.R. and Sulman, B.N., 2017. Wetland flux
622   controls: how does interacting water table levels and temperature influence
623   carbon   dioxide   and   methane   fluxes   in   northern   Wisconsin?
624   Biogeochemistry.
625   Pumpanen, J. et al., 2004. Comparison of different chamber techniques for
626   measuring soil CO_2 efflux. Agricultural and Forest Meteorology, 123(3):
627   159-176.
628   Raich, J.W., Potter, C.S. and Bhagawati, D., 2010. Interannual variability in
629   global soil respiration, 1980-94. Global change biology, 8(8): 800-812.
630   Reth, S., Reichstein, M. and Falge, E., 2005. The effect of soil water content,
631   soil temperature, soil pH-value and the root mass on soil CO_2 efflux – a
632   modified model. Plant and soil, 268(1): 21-33.
633   Rodríguez, J.F., Saco, P.M., Sandi, S., Saintilan, N. and Riccardi, G., 2017.
634   Potential increase in coastal wetland vulnerability to sea-level rise
635   suggested by considering hydrodynamic attenuation effects. Nature
636   Communications, 8: 16094.
637   Sánchez-Cañete, E.P., Scott, R.L., van Haren, J. and Barron-Gafford, G.A.,
638   2017. Improving the accuracy of the gradient method for determining soil
639   carbon dioxide efflux. Journal of Geophysical Research: Biogeosciences,
640   122(1): 50-64.
641   Smith, C., DeLaune, R. and Patrick Jr, W., 1983. Carbon dioxide emission and
642   carbon accumulation in coastal wetlands. Estuarine, coastal and shelf
643   science, 17(1): 21-29.
644   Song, C., Xu, X., Tian, H. and Wang, Y., 2009. Ecosystem–atmosphere
645   exchange of CH_4 and N_2O and ecosystem respiration in wetlands in the
646   Sanjiang Plain, Northeastern China. Global change biology, 59(3): 692-705.
647   Song, W. et al., 2015. Methane emissions from an alpine wetland on the Tibetan

Biogeosciences
Discussions

Open Access

EGU

648   Plateau: Neglected but vital contribution of the nongrowing season. Journal
649   of Geophysical Research Biogeosciences, 120: 1475-1490.
650 St-Hilaire, F. et al., 2010. McGill Wetland Model: evaluation of a peatland
651   carbon simulator developed for global assessments. Biogeosciences
652   Discussions, 7(11): 3517-3530.
653 Wang, G. and Chen, S., 2012. A review on parameterization and uncertainty in
654   modeling greenhouse gas emissions from soil. Geoderma, 170: 206-216.
655 Wang, G.D., Wang, M., Lu, X.G. and Jiang, M., 2016. Surface elevation change
656   and susceptibility of coastal wetlands to sea level rise in Liaohe Delta,
657   China. Estuarine Coastal & Shelf Science, 180: 204-211.
658 Wanninkhof, R. and Knox, M., 2003. Chemical enhancement of CO_2 exchange
659   in natural waters. Limnology & Oceanography, 41(4): 689-697.
660 White, J.R., Delaune, R.D., Roy, E.D. and Corstanje, R., 2014. Uncertainty In
661   Greenhouse Gas Emissions On Carbon Sequestration In Coastal and
662   Freshwater Wetlands of the Mississippi River Delta: A Subsiding Coastline
663   as a Proxy for Future Global Sea Level, AGU Fall Meeting.
664 Wolkovich, E.M., Cook, B.I. and Davies, T.J., 2014. Progress towards an
665   interdisciplinary science of plant phenology: building predictions across
666   space, time and species diversity. New Phytologist, 201(4): 1156.
667 Wu, J. et al., 2017. Partitioning controls on Amazon forest photosynthesis
668   between environmental and biotic factors at hourly to interannual
669   timescales. Global change biology, 23(3): 1240.
670 Xie, X., Zhang, M.Q., Zhao, B. and Guo, H.Q., 2014. Dependence of coastal
671   wetland ecosystem respiration on temperature and tides: a temporal
672   perspective. Biogeosciences, 11(3): 539-545.
673 Xu, X. et al., 2014. Seasonal and spatial dynamics of greenhouse gas
674   emissions under various vegetation covers in a coastal saline wetland in
675   southeast China. Ecological Engineering, 73: 469-477.
676 Yang, G. et al., 2014. Effects of soil warming, rainfall reduction and water table
677   level on CH_4 emissions from the Zoige peatland in China. Soil Biology and
678   Biochemistry, 78(0): 83-89.
679 Ye, S. et al., 2016. Inter-Annual Variability of Area-Scaled Gaseous Carbon
680   Emissions from Wetland Soils in the Liaohe Delta, China. PLoS ONE, 11(8).
681 Yuste, J.C., Janssens, I.A. and Ceulemans, R., 2005. Calibration and validation
682   of an empirical approach to model soil CO_2 efflux in a deciduous forest.
683   Biogeochemistry, 73(1): 209-230.
684 Zhang, Q., Sun, R., Jiang, G., Xu, Z. and Liu, S., 2016. Carbon and energy flux
685   from a Phragmites australis wetland in Zhangye oasis-desert area, China.
686   Agricultural and Forest Meteorology, 230–231: 45-57.
687